

NMR Observation of Poly(ethylene oxide) Dynamics in a Poly(methyl methacrylate) Matrix. Effect of Chain Length Variation

C. Brosseau, A. Guillermo, and J. P. Cohen-Addad*

Laboratoire de Spectrométrie Physique,[†] Université Joseph Fourier, B.P. 87, 38402 Saint-Martin-d'Hères Cedex, France

Received September 16, 1991; Revised Manuscript Received April 13, 1992

ABSTRACT: The molecular weight dependence of the proton transverse nuclear magnetic relaxation rate of poly(ethylene oxide) (PEO) blended with deuterated poly(methyl methacrylate) (PMMA) of molecular weight 5.1×10^4 is reported. Two domains of chain dynamics are observed in the molten state. For PEO molecular weights M_w less than 2.5×10^4 , the chain length dependence of the relaxation rate $1/T_2$ scales as M_w^β with $\beta \approx 0.9$. For higher molecular weights ($2.5 \times 10^4 < M_w < 6.5 \times 10^4$) the data are analyzed by assuming a partition of each chain into submolecules. These submolecules have a molecular weight which is close to that of the submolecule, $M_s \approx 7 \times 10^3$, derived from the plateau modulus measurement of this mixture at the same concentration and already reported in the literature.

I. Introduction

Since the pioneering work of Slichter and Davis, it is now well established that NMR is sensitive to the presence of entanglements in high molecular weight polymer melts.¹ The magnetic relaxation of nuclei can be used both to characterize temporary network structures formed by entanglements and to probe semilocal properties of chain dynamics.^{2,3} Transverse relaxation processes of protons, ¹³C nuclei, and deuterium nuclei attached to polymers exhibit a behavior specific to the presence of transient network structures whereas the spin-lattice relaxation demonstrates the existence of fast local motions of segments.^{4,5}

This work deals with the observation of the dynamics of poly(ethylene oxide) (PEO) chains moving in a molten blend formed with deuterated poly(methyl methacrylate) (PMMA) chains. Two main questions arise from studies of chain dynamics in polymer blends.

(i) The first one concerns the definition of a temporary network structure. This key property is now well characterized in any simple high molecular weight polymeric liquid; it gives rise to the effect of temporary elasticity represented by a plateau of the relaxation modulus $G(t)$. The value of the plateau G°_N is specific to each polymer. Although this effect is well defined experimentally, it has not been given any quantitative description except for a recent model proposed by Iwata and Edwards.⁶ The description of polymer dynamics is based on the partition of one chain into submolecules. The mean molecular weight M_e of one submolecule is given by

$$M_e = \rho RT / G^\circ_N \quad (1)$$

ρ being the pure polymer density and $R = 8.31 \text{ J K}^{-1} \text{ mol}^{-1}$.

The migration process of one chain arises from the collective motions of these submolecules while it is considered that long-range fluctuations are screened within submolecules. In other words, segmental motions are not chain length dependent. The definition of a transient network in a blend made from A and B polymers characterized by their own transient network structures has not been given any quantitative description, although a modulus of elasticity $G^\circ_N(A,B)$ can be determined experimentally. It varies continuously from $G^\circ_N(A)$, cor-

responding to the pure A polymer, to $G^\circ_N(B)$, corresponding to the pure B polymer. It is of interest to know whether each chain participates in a single transient network structure of A and B submolecules characterized by a single mean molecular weight.⁷

$$M_e(A,B) = \rho RT / G^\circ_N(A,B) \quad (2)$$

Then, this partition of polymers should underly the long-range dynamics of chains. Another possibility is to assume the existence of two temporary network structures in a blend. It has been suggested that the appearance of entanglements of A chains occurs when their chain molecular weight is higher than the characteristic mass defined by M_c^A / ϕ_A , where M_c^A is the characteristic mass of the pure A polymer and ϕ_A is its volume fraction in a blend AB.⁸ However, this empirical law has not yet been given any theoretical support.

(ii) The second question concerns the nature of chain dynamics. It is now well-known that the Rouse model accounts for dynamical properties of short chains in a melt; the chain molecular weight M must be less than the characteristic mass M_c . Then the zero shear rate viscosity η_0 is expressed as

$$\eta_0 = \rho RT T_r / M \quad (3)$$

T_r being the terminal relaxation time of a single chain in a melt; T_r is a function of the molecular weight:

$$T_r \sim \zeta_0 M^2 \quad (3')$$

where ζ_0 defines a local friction coefficient which is sensitive to free volume variations in the polymeric liquid. When the molecular weight is higher than M_c , the tube concept is introduced to account for the hindrance that affects the lateral diffusion of one chain, i.e., the diffusion perpendicular to the direction of the chain backbone.⁹ The terminal relaxation time T_r is predicted to be proportional to M^3 while the translational diffusion coefficient D_s exhibits an M^{-2} dependence.

In the case of A and B polymers in a blend, it is of importance to determine the nature of chain dynamics of each species. According to the recent experimental approach reported by Composto et al.,¹⁰ the tracer diffusion coefficient of deuterated polystyrene in protonated blends of this polymer and poly(2,6-dimethyl-1,4-phenylene oxide), also named poly(xylenyl ether), was measured using

* Laboratoire associé au CNRS.

forward-recoil spectrometry and was found to vary as M^{-2} for $M > 1.9 \times 10^4$ (where M is the tracer molecular weight) independent of the matrix molecular weights investigated, suggesting that the tracer diffusion occurs by reptation.

In this work, properties of PEO/PMMA blends are probed from PEO chains by observing the proton transverse relaxation of PEO; PMMA chains are deuterated to eliminate any ambiguity in the interpretation of NMR results. A single concentration of PEO is used. The purpose of this study is twofold. (i) It is first attempted to determine whether PEO chains participate in any transient network structure. (ii) It is then attempted to determine the nature of the dynamics of PEO chains by varying the polymer molecular weight from 0.4×10^4 to 6.5×10^4 while the PMMA molecular weight is kept constant ($M = 5.1 \times 10^4$). All NMR measurements were performed at temperatures well above the glass transition temperature of the blends.

II. Principle of the NMR Approach

The principle of the NMR approach is based upon the search for a pseudosolid behavior of the transverse magnetic relaxation of protons attached to polymer chains.

(i) In the case of long polymer chains ($M_w > 10^5$) observed well above the glass transition in a melt, the transverse magnetization behaves as in a permanent gel because of the existence of a temporary network structure. Entanglements induce temporary topological constraints that hinder the rotational diffusion of monomeric units. The relaxation time of these topological constraints has the same order of magnitude as the terminal time T_r , which is proportional to M^3 . During time intervals shorter than T_r , monomeric units undergo nonisotropic motions which give rise to a nonzero average of dipole-dipole interactions of spins $\langle \mathcal{H}_T \rangle_R$. The effect of anisotropy is relaxed over time intervals longer than T_r ; the terminal time T_r is also a measure of the lifetime of the residual interaction of spins $\langle \mathcal{H}_T \rangle_R$.¹¹ According to the description of the motional averaging effect which applies to any nuclear spin system in a liquid, the residual interaction is observed whenever the following condition is fulfilled: $\langle \mathcal{H}_T \rangle_R T_r > 1$. Then the magnetization dynamics is fully governed by the residual interaction $\langle \mathcal{H}_T \rangle_R$. The dynamics of monomeric unit motions is not detected; NMR is only sensitive to the degree of asymmetry of local motions. This relaxation process specific to long polymer chains is well described elsewhere.¹² They arise from a pulse sequence $90^\circ(y) - \tau - 180^\circ(y) - \tau - 90^\circ(-x)$. They exhibit several characteristic properties which permit one to disclose the presence of a residual interaction of spins without any ambiguity.

(ii) A motional averaging effect of the residual interaction $\langle \mathcal{H}_T \rangle_R$ starts being observed when $\langle \mathcal{H}_T \rangle_R$ and the terminal relaxation rate T_r^{-1} are such that $\langle \mathcal{H}_T \rangle_R < T_r^{-1}$.

(iii) Finally, a full motional averaging effect is observed in the case of short polymer chains. This situation is analyzed in the following way. The estimate of the residual interaction of spins associated with one short chain which contains N skeletal bonds is given by $|\mathcal{H}_T|/N$. The terminal relaxation time T_r is derived from eq 3. Then a full motional averaging effect is observed when the following condition is fulfilled:

$$|\mathcal{H}_T| \eta_0 M_b / \rho RT < 1 \quad (4)$$

M_b being the molecular weight of one skeletal bond. This gives the limiting value of the viscosity η_0 : $\eta_0 < \rho RT / |\mathcal{H}_T| M_b$; i.e., $\eta_0 < 500$ Pa·s. The relaxation rate of the

Table I
Physical Parameters Characterizing PEO and PMMA^a

	PEO	PMMA
M_c^b	3600	31000
M_e	2200	9100
G_N^b (10^7 dyn cm ⁻²)	1.8 (453 K)	0.48 (473 K), 0.62 (423 K)
C_∞^b	3.8	8.7
T_g (K)	218	378
ρ^b (g cm ⁻³)	1.08	1.14
l^b (Å)	1.49	1.54

^a M_c is the characteristic molecular weight, M_e is the mean molecular weight between entanglements, G_N^b is the viscoelastic plateau modulus, C_∞ is the characteristic ratio, T_g is the glass transition temperature, ρ is the density, and l is the mean bond length. ^b Values are taken from ref 18.

transverse magnetization of protons is defined from the correlation function of the spin dipolar interaction:¹¹

$$\Gamma(t) = 3 \langle (2Z^2(0) - X^2(0) - Y^2(0))(2Z^2(t) - X^2(t) - Y^2(t)) \rangle / 4 \langle \mathbf{R}^2 \rangle^2 \quad (5)$$

$$\Gamma(t) = 9 \langle (Z^2(0) Z^2(t)) - \langle Z^2(t) \rangle^2 \rangle / 2 \langle \mathbf{R}^2 \rangle^2 \quad (6)$$

X , Y , and Z are the coordinates of the end-to-end vector \mathbf{R} and $\Gamma(0) = 1$. The correlation function is simply expressed as the square of the end-to-end vector correlation:¹¹ $\Gamma(t) = C^2(t)$,

$$C(t) = (8/\pi^2) \sum_{p=\text{odd}} \frac{1}{p^2} \exp(-t/2\tau_p) \quad (7)$$

For the Rouse model¹³ the relaxation time τ_p is given by

$$\tau_p = \langle \mathbf{R}^2 \rangle N \zeta_0 / 6\pi^2 k T_p^2 \quad p = 1, 2, \dots \text{ and } p \ll N$$

$\langle \mathbf{R}^2 \rangle$ being the mean square end-to-end distance of the chain.

The friction coefficient may exhibit a molecular weight dependence induced by the free volume associated with the chain ends. The magnetic relaxation rate of protons reads

$$\frac{1}{T_2} \sim |\mathcal{H}_T|^2 / N^2 \int_0^\infty \Gamma(t) dt \quad (8)$$

or

$$\frac{1}{T_2} \sim |\mathcal{H}_T|^2 / N^2 \sum_{p,q \text{ odd}} 2p^{-2}q^{-2} \left(\frac{1}{\tau_p} + \frac{1}{\tau_q} \right)^{-1} \quad (9)$$

The series expansion is dominated by the first term corresponding to $p = 1$ and $q = 1$, yielding

$$\frac{1}{T_2} \sim |\mathcal{H}_T|^2 \tau_1 / N^2 \quad (9')$$

with $\tau_1 = T_r$, or

$$\frac{1}{T_2} \sim |\mathcal{H}_T|^2 \langle \mathbf{R}^2 \rangle \zeta_0 / 6\pi^2 k T N \quad (10)$$

It is seen from the above equation that for a Gaussian chain the molecular weight dependence of the relaxation rate $1/T_2$ arises only from the friction coefficient ζ_0 .

III. Experimental Section

Information about the polymers used in this work is provided in Table I. Deuterated PMMA has a molecular weight equal to 5.1×10^4 with a polydispersity index of 1.06. The value of the average molecular weight which defines the mean spacing between entanglements is estimated from the modulus of temporary elasticity G_N^b (from eq 1). The number of subchains is about 6. PEO has a molecular weight average ranging from 0.42×10^4

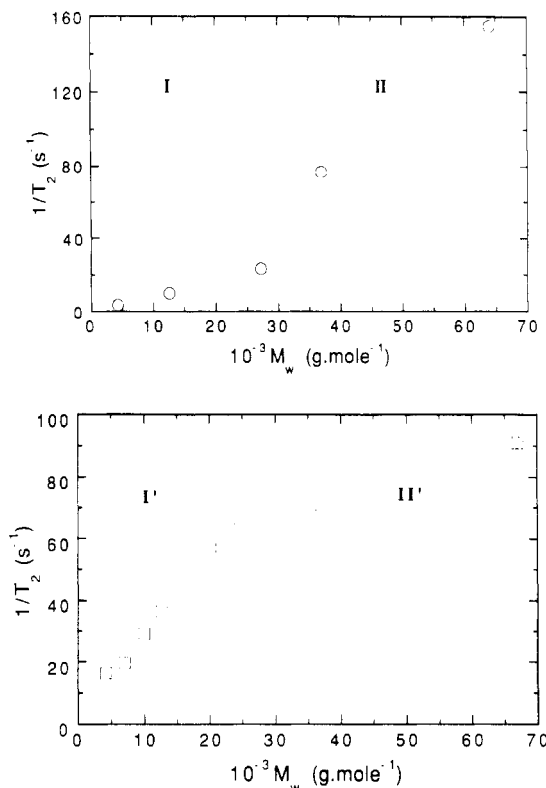


Figure 1. (a, Top) Proton NMR relaxation rate $1/T_2$ (s^{-1}) of pure PEO plotted against PEO molecular weight. $T = 358$ K ($T - T_g = 140$ K). (b, Bottom) Relaxation rate $1/T_2$ (s^{-1}) of PEO in a PEO/PMMA(D) blend plotted against PEO molecular weight. The PEO concentration is 20% in weight, $M_w(\text{PMMA}) = 5.1 \times 10^4$, and $T = 426$ K ($T - T_g = 100$ K).

to 6.5×10^4 with polydispersity indexes of less than 1.10. $M_w(\text{PEO})$, which defines the mean spacing between entanglements in a pure PEO melt, is equal to 2.2×10^3 . These polymers were purchased from Polymer Laboratories.

Samples containing 20% in mass of PEO were prepared according to a procedure already described in detail.¹⁴ Measurements on the blend were made at 426 K, corresponding to the glass transition temperature¹⁴ of these blends shifted upward of 100 K. The mixture is in the single-phase regime since recent small-angle neutron scattering measurements by Russell and co-workers¹⁵ reveal that this blend exhibits a lower critical solution temperature at 500 K. Measurements on pure PEO were made at $T = 358$ K ($T_g + 140$ K), which is above the melting temperature $T_m = 338$ K.

The nuclear transverse relaxation functions $M_x(t)$ were measured by spin-echo sequences. In accordance with the purpose put forward in section II, a pseudosolid echo (denoted $E(t, \tau)$) sequence as described elsewhere¹² was also employed to probe the motional averaging of the residual dipolar interaction by chain dynamics. The experiments depicted in this study were carried out on a pulsed CXP Bruker spectrometer operating at 36 MHz.

IV. Proton Transverse Relaxation in Pure PEO

It is worth illustrating properties of the transverse relaxation in pure PEO before analyzing the behavior of the proton magnetization observed on PEO in blends. Starting from short chains, two main domains can be defined. This behavior is illustrated in Figure 1a without entering into details of analysis. Within the first domain, hereafter called I, no pseudosolid spin echoes are observed. The magnetic relaxation rate exhibits a weak molecular weight dependence. In the second domain, hereafter called

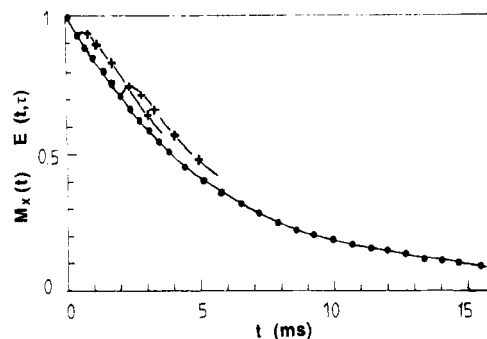


Figure 2. Relaxation function $M_x(t)$ (\bullet) and pseudosolid echoes $E(t, \tau)$ ($+$) observed from pure PEO. $M_w = 6.5 \times 10^4$, $T = 358$ K. Solid and dashed lines are guides to the eyes.

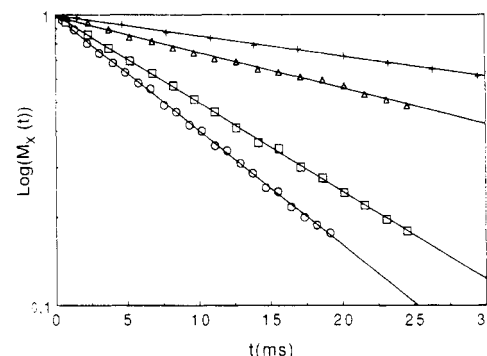


Figure 3. Semilogarithmic plot of the relaxation functions of PEO/PMMA(D) blend. Weight concentration of PEO is 20%, $T = 426$ K, and $M_w(\text{PMMA}) = 5.1 \times 10^4$. ($+$) $M_w(\text{PEO}) = 4.3 \times 10^3$; (Δ) $M_w(\text{PEO}) = 10^4$; (\square) $M_w(\text{PEO}) = 3.7 \times 10^4$; (\circ) $M_w(\text{PEO}) = 6.5 \times 10^4$. Solid lines indicate exponential fits.

II, pseudosolid echoes start being observed although they have weak amplitudes. This can be seen in Figure 2, where pseudosolid echoes have been drawn at two fixed time values ($\tau = 0.5$ ms and $\tau = 2$ ms). The motional narrowing effect induced by chain motion becomes only partial because of the presence of a temporary network structure. A strong molecular weight dependence is observed; it is associated with the lifetime T_f of entanglements. An analysis of this typical molecular weight dependence of the transverse relaxation rate observed for other polymers has been already proposed.³

V. Proton Transverse Relaxation of PEO in Blends

In this section it is shown that the proton transverse relaxation of PEO in molten blends is very contrasted to that of PEO in a pure melt.

1. Characteristic Features. Three main features characterize the proton transverse relaxation process observed from PEO chains in blends.

(a) Exponential Relaxation. To detect the possible effect of the presence of entanglements upon the proton transverse relaxation, the PEO molecular weight was varied from 0.4×10^4 to 6.5×10^4 . The irreversible dynamics of the transverse magnetization can be represented by a single-exponential time function (see Figure 3; for the sake of clarity only four curves have been drawn) characterized by a spin-spin relaxation time T_2 which varies from 11 to 61 ms.

(b) No Pseudosolid Behavior. No pseudosolid behavior of the magnetization was detected by applying pseudosolid echo sequences. These sequences were found to give rise to a spin-system response in coincidence with the relaxation function observed from usual Hahn spin echoes. This surprising property shows that spin-spin interactions

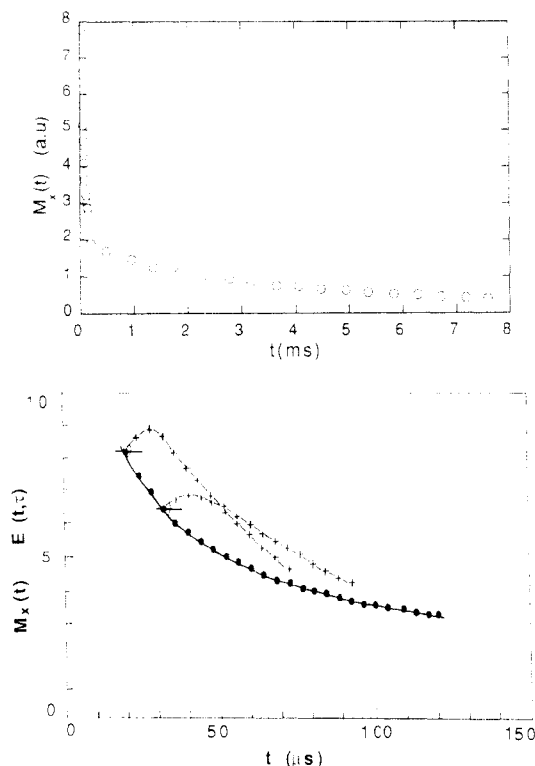


Figure 4. (a, Top) Relaxation function $M_x(t)$ (○) for a PEO-(H)/PMMA(H) blend (PEO weight concentration of 20%). $T = 426$ K ($T - T_g = 100$ K), $M_w(\text{PMMA}) = 6 \times 10^4$, and $M_w(\text{PEO}) = 2.2 \times 10^4$. (b, Bottom) pseudosolid echoes $E(t, \tau)$ (+) corresponding to PMMA(H). Solid and dashed lines are guides to the eyes.

of PEO protons are fully averaged by chain motions in this blend. This experimental result holds even for chain molecular weights where pseudosolid echoes are obtained in a pure PEO melt. Consequently, PEO relaxation functions in blends yield information about properties of pure chain dynamics.

The temperature and molecular weight dependences of the PEO pseudosolid behavior were further appreciated in an earlier work:¹⁴ $T = 426$ K corresponds to the lowest temperature for which no pseudosolid echoes are detected for the highest molecular weight investigated here. Therefore, at this step of the analysis of the experimental results two hypotheses may be considered. Either PEO chains do not participate in any temporary network structure or they form entanglements but have a lifetime which is too short to be observed from NMR.

This contrasts with the NMR properties of PMMA investigated in a PEO(H)/PMMA(H) blend ($M_w(\text{PEO}) = 2.2 \times 10^4$) at 426 K. The long decay of the relaxation function displayed in Figure 4a corresponds to the protons of PEO chains. The short decay associated with the protons of PMMA chains is characterized by well-shaped pseudosolid echoes (Figure 4b): this indicates that the PMMA chains participate in a network structure.

(c) **Two Chain Dynamics Domains.** It is clearly seen from Figure 1b that two domains of chain dynamics can be determined. The crossover between the two domains occurs when the chain molecular weight is about 2.5×10^4 . Within the first domain, the relaxation rates measured in pure PEO and in blends take a similar molecular weight dependence (Figure 5). On the contrary, as shown in Figure 1, the relaxation rates in domains II and II' behave very differently.

2. Short-Chain Dynamics. Within domain I', the apparent chain molecular weight dependence of the relaxation rate is well represented by $1/T_2 \propto M^{0.86 \pm 0.06}$

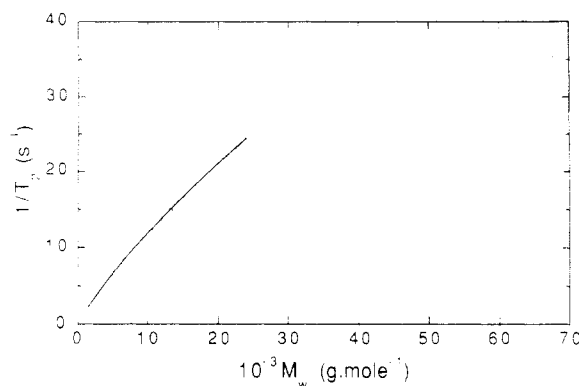


Figure 5. Relaxation rates $1/T_2$ (s^{-1}) of pure PEO (○) and PEO in PEO/PMMA(D) blend (□) plotted at a constant shift from the glass transition temperature ($T - T_g = 140$ K). Solid line represents a power law fit $M^{0.86 \pm 0.06}$ of the data in the domain I'.

(Figure 5). In this figure, the relaxation rates of pure PEO and of PEO blended with PMMA are compared at $T - T_g = 140$ K. This temperature correction was computed by using the WLF law, which governs the transverse relaxation rate of PEO in the molten PEO/PMMA(D) blend.¹⁴ Let us note that at $T - T_g = 140$ K the value of the relaxation rate of PEO in the blend is close to that measured in pure PEO. This remark agrees with the fact that for a constant value of $T - T_g$ the fractional free volume of PEO is slightly affected when PEO is blended with PMMA.^{14,16}

This molecular weight dependence agrees with the recent experimental study reported by Cheng et al.¹⁷ showing that the self-diffusion coefficient D_s of PEO chains decreases as $D_s \sim M^{-1.85 \pm 0.02}$ for similar chain lengths. Correspondingly, the terminal relaxation time is expected to vary as $M^{2.85}$ instead of M^2 . The discrepancy between the experimental value of the exponent and the value predicted from the Rouse model has been ascribed to a free volume effect induced by chain ends.¹⁷ Substituting the dependence $\tau_1 \sim N^{2.85}$ into eq 9' gives $1/T_2 \sim |\mathcal{H}_T|^2 N^{0.85}$, in accordance with experimental results within the uncertainty of measurements (Figure 5).

In the case of pure PEO, an estimate of the relaxation rate $1/T_2$ can be calculated from eq 9' with $|\mathcal{H}_T| = 10^5 \text{ s}^{-1}$. The correlation time τ_1 was derived from measurements of the diffusion coefficient D : $\tau_1 = \langle R^2 \rangle / 6D_s$ with $\langle R^2 \rangle = C_\infty N j l^2$, where j denotes the number of skeletal bonds per monomer ($j = 3$), and l and C_∞ are given in Table I. Then from the results of ref 17, we found that $\tau_1 = 1.2 \times 10^{-5}$ s and $1/T_2 = 5 \text{ s}^{-1}$ at 358 K (i.e., $T - T_g = 140$ K) and for $M_w = 9 \times 10^3$; this estimate is in good accordance with the experimental data (Figure 5).

The observed chain length dependence implies that long-range chain properties are involved in the relaxation process of the transverse magnetization.

3. Submolecule Dynamics. The slow variation of the relaxation rate $1/T_2$ in domain II' ($M > 2.5 \times 10^4$) implies the partition of any chain into submolecules. This is shown in the following way. Each submolecule is formed from N_s skeletal bonds. The residual interaction of spins must be calculated over one submolecule; its estimate is given by $|\mathcal{H}_T|/N_s$. It is postulated that these submolecules have a physical evidence like the mean spacing between entanglements in a pure melt for instance. Submolecules introduced in the Rouse model have no physical existence but they help to establish the description of low-frequency fluctuations in one chain. Once the partition of one chain is postulated, a framework of description of collective motions of submolecules must be used to relate long-range fluctuations in one chain to the mechanisms of transverse magnetic relaxation.¹¹

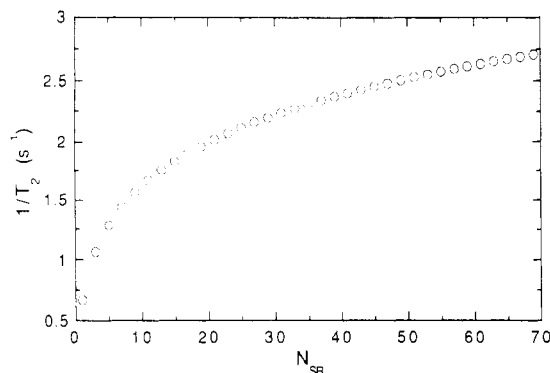


Figure 6. Theoretical dependence of the magnetic relaxation rate $1/T_2$ as a function of the number N_{sr} of the Rouse submolecules according to eq 12. In the numerical calculations, we have set $|\mathcal{H}_T|^2 = 1 \text{ s}^{-2}$.

Two spectra of chain relaxation have been used until now to interpret NMR results. One of them is associated with the Rouse model while the other one is derived from the reptation motion of one chain in its tube.⁹ In this work, the magnetic relaxation is related to the Rouse model, according to which the following equation applies in the case of a full motional averaging effect:¹¹

$$\frac{1}{T_2} = \langle (\mathcal{H}_T)_R \rangle^2 \frac{1}{N_{sr}^2} \sum_{p,q=1}^{N_{sr}} \left(\frac{1}{\tau_p} + \frac{1}{\tau_q} \right)^{-1} \quad (11)$$

with $N_{sr} = N/N_s$ denoting the number of Rouse submolecules.

Now inserting the molecular weight dependence of τ_p and the estimate of $\langle \mathcal{H}_T \rangle_R$ into eq 11, it follows

$$\frac{1}{T_2} \sim \frac{|\mathcal{H}_T|^2}{N_{sr}^2} \sum_{p,q=1}^{N_{sr}} \frac{1}{\sin^2 \left(\frac{\pi p}{2N_{sr} + 1} \right) + \sin^2 \left(\frac{\pi q}{2N_{sr} + 1} \right)} \quad (12)$$

with $1/\tau_p \sim N_s^{-2} \sin^2 [\pi p / (2N_{sr} + 1)]$. From eq 12, the N_{sr} dependence of the magnetic relaxation rate is depicted in Figure 6. The molecular weight dependence of $1/T_2$ observed in domain II' is now compared to Figure 6 according to the following procedure. We first adjusted the actual increase in domain II' with the variation predicted in Figure 6 for a ratio of N_{sr} equal to the ratio of M_w corresponding to domain II'. Moreover, the computed values of the relaxation rate are referred to the experimental value at $M_w = 2.5 \times 10^4$ which separates domains I' and II'. The experimental data are well described by the assumption of chain partition as expressed by eq 12 and a value of N_s yielding a molecular weight M_s of the submolecule larger than 2×10^3 (dashed line in Figure 7). A better representation is obtained by taking $M_s = 10^4$ (solid line). This partition implies that the average number of submolecules is about 2 at the frontier between domains I' and II'. This low value agrees with the analysis of the relaxation rate in the short-chain domain I' for which the motional averaging condition originates from the terminal relaxation mode of the entire chain.

VI. Discussion and Concluding Remarks

Now returning to the two purposes of this work, two comments are in order.

(1) The chain partition evidenced in domain II' yields a submolecule of molecular weight M_s having a typical value of the molecular weight M_e of a viscoelastic sub-chain. Moreover, the experimental data are better de-

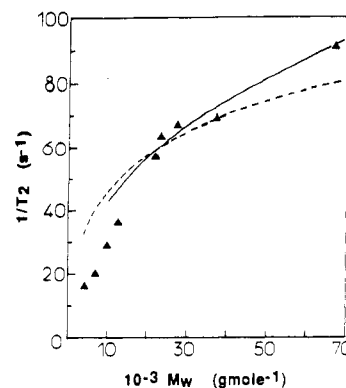


Figure 7. Relaxation rate $1/T_2$ of PEO in a PEO/PMMA(D) blend. The lines are fits of the data in domain II' according to eq 12 with $M_s = 10^4$ (solid line) and $M_s = 2 \times 10^3$ (dashed line).

scribed (Figure 7) with M_s close to M_e (PMMA) instead of M_e (PEO). Pseudosolid echoes observed on PMMA(H) in protonated blends (Figure 4b) indicate the existence of a temporary network. These observations lead one to associate the chain partition M_s with this network in the blend. On the basis of viscoelastic plateau measurements, Wu⁷ and Tsenoglou¹⁹ have computed the molecular weight M_e characterizing the network of PEO/PMMA blends as a function of the concentration and found respectively $M_e = 7.4 \times 10^3$ and $M_e = 6.25 \times 10^3$ for ϕ (PEO) = 0.20. The value of Wu was computed thanks to eq 1 assuming that G°_N is given by

$$G^\circ_N(A,B) = \phi_A G^\circ_N(A) + \phi_B G^\circ_N(B) + \phi_A \phi_B (\lambda_e - 1) [G^\circ_N(A) + G^\circ_N(B)] \quad (13)$$

with ϕ_j ($j = A, B$) the volume fraction of the j th component and $\lambda_e = 0.512$ for the PEO/PMMA couple.⁷ That of Tsenoglou was derived from eq 1 taking G°_N as

$$[G^\circ_N(A,B)]^{1/2} = \phi_A [G^\circ_N(A)]^{1/2} \left(1 + \epsilon \frac{\phi_B [G^\circ_N(B)]^{1/2}}{\phi_A [G^\circ_N(A)]^{1/2}} \right)^{1/2} + \phi_B [G^\circ_N(B)]^{1/2} \left(1 + \epsilon \frac{\phi_A [G^\circ_N(A)]^{1/2}}{\phi_B [G^\circ_N(B)]^{1/2}} \right)^{1/2} \quad (14)$$

with $\epsilon = 0.17$ for the PEO/PMMA couple.¹⁹

(2) The last issue we will discuss concerns the monomeric friction coefficient. Figure 4a indicates that $1/T_2$ -(PEO) is much different from $1/T_2$ -(PMMA) for that concentration and at the temperature explored. This reflects a higher mobility of the PEO chains than the PMMA chains in that homogeneous blend. Measurements of $T_{1\rho}$ (¹H) in the same blends²⁰ have shown that this effect is due to a large difference of segmental motion rates of these two polymers in the high-frequency range (i.e., around 52 kHz). This means that even in the single-phase regime, components of a binary blend may keep their dynamical characteristics. This is a similar result to that reported by Composto et al.¹⁰ in miscible PS/PXE blends by determining the monomeric friction coefficients through measurements of self-diffusion coefficients. They found that $\zeta_0(\text{PS}) \ll \zeta_0(\text{PXE})$ for each concentration and that the rate at which a PS molecule moves is much greater than that of a PXE molecule, even though both chains are diffusing in identical surroundings. It would be interesting to measure the monomeric friction coefficients in high molecular weight blends of PEO/PMMA in like fashion as was done by Composto et al.¹⁰ to see whether this blend possesses the same behavior as PS/PXE.

Acknowledgment. Financial support from Atochem is greatly acknowledged. We thank Dr. M. Audenaert for useful discussions.

References and Notes

- (1) Slichter, W. P.; Davis, D. D. *J. Appl. Phys.* **1963**, *34*, 98.
- (2) Cohen-Addad, J. P. *J. Chem. Phys.* **1974**, *60*, 2440.
- (3) Cohen-Addad, J. P.; Guillermo, A. *J. Polym. Sci., Polym. Phys. Ed.*, **1984**, *22*, 931. Cohen-Addad, J. P.; Dupeyre, R. *Macromolecules* **1985**, *18*, 1101.
- (4) Dejean de la Batie, R.; Laupretre, F.; Monnerie, L. *Macromolecules* **1989**, *22*, 2052.
- (5) Guillermo, A.; Dupeyre, R.; Cohen-Addad, J. P. *Macromolecules* **1990**, *23*, 1291.
- (6) Iwata, K.; Edwards, S. F. *J. Chem. Phys.* **1989**, *90*, 4567.
- (7) Wu, S. *J. Polym. Sci., Polym. Phys. Ed.* **1987**, *25*, 2511.
- (8) Watanabe, H.; Kotaka, T. *Macromolecules* **1984**, *17*, 2316.
- (9) de Gennes, P.-G. *J. Chem. Phys.* **1971**, *55*, 572.
- (10) Composto, R. J.; Kramer, E. J.; White, D. M. *Polymer* **1990**, *31*, 2320.
- (11) Cohen-Addad, J. P. *J. Phys. (Paris)* **1982**, *43*, 1509.
- (12) Cohen-Addad, J. P.; Schmit, C. *Polymer* **1988**, *29*, 883.
- (13) Graessley, W. W. *Advances in Polymer Science*; Springer-Verlag: Berlin, 1974.
- (14) Brosseau, C.; Guillermo, A.; Cohen-Addad, J. P. *Polymer*, in press.
- (15) Russell, T. P.; Ito, H.; Wignall, G. D. *Macromolecules* **1988**, *21*, 1703. Ito, H.; Russell, T. P.; Wignall, G. D. *Macromolecules* **1987**, *20*, 2213.
- (16) Colby, R. H. *Polymer* **1989**, *30*, 1275.
- (17) Cheng, S. Z. D.; Barley, J. S. Von Meerwall, E. D. *J. Polym. Sci., Polym. Phys. Ed.* **1991**, *29*, 515.
- (18) Graessley, W. W.; Edwards, S. F. *Polymer* **1981**, *22*, 1329.
- (19) Tsenoglou, C. *J. Polym. Sci., Polym. Phys. Ed.* **1988**, *26*, 2329.
- (20) Guillermo, A.; Brosseau, C.; Cohen-Addad, J. P. *Polymer*, submitted.

Registry No. PEO, 25322-68-3; PMMA (homopolymer), 9011-14-7.